Preparation of Polymer–Ceramic Composite Membranes with Thin Defect-Free Separating Layers

M. E. REZAC and W. J. KOROS*

The University of Texas at Austin, Department of Chemical Engineering, Austin, Texas 78712-1062

SYNOPSIS

Polymer–ceramic composite membranes with essentially defect-free separating layers have been prepared by a solution deposition technique. Rigid polymers were used for the selective organic layer. These included high molecular weight samples of 5,5'-[2,2,2-trifluoro-1-(trifluoromethyl)ethylidene]bis-1,3-isobenzofuran-dione, isopropylidenedianiline (6FDA-IPDA), 5,5'-[2,2,2-trifluoro-1-(trifluoromethyl)ethylidene]bis-1,3-isobenzofuran-dione, methylenedianiline (6FDA-MDA), tetramethylhexafluorobisphenol-A polycarbonate (TMHFPC), and tetramethylhexafluoropolysulfone (TMHFPSF). Attempts to prepare composite membranes from lower molecular weight samples of bisphenol-A polycarbonate (PC) and tetrabromohexafluorobisphenol-A polycarbonate (TBHFPC) were unsuccessful. The PC and TBHFPC composites exhibited a decrease in the measured gas flux after polymer deposition; however, the selectivities of the composites were considerably less than that of a dense film of the same materials. A microporous ceramic membrane prepared by Anotec Separations was used as the support layer. This ceramic membrane provided minimal resistance to gas flow. The selective composite membranes were found to have high gas fluxes and gas separating abilities essentially equivalent to that of a dense isotropic film. The estimated, effective skin layer thicknesses for these membranes are on the order of 1500 Å to 1.0 μm. The formation of these composites is believed to occur through a sieving process in which large swollen polymer chains are sieved out of solution by the ceramic support. Polymer solutions that had swollen coil diameters that were smaller than that of the ceramic membrane did not produce selective composite membranes, while those solutions with swollen coil diameter that were larger than that of the ceramic membrane produced defect-free polymer layers.

INTRODUCTION

In principle, composite membranes offer advantages over asymmetric polymeric membranes in that the properties of both the dense separating layer and the porous support layer can be individually optimized. For maximum productivity in a minimum sized separating unit, an ultrathin defect-free separating layer is required. In practice, the production techniques that have been employed for the production of composite membranes limit the size of the pores and the degree of porosity that can be used in the support. Typically, these values have been small. If the pore size was too large, achieving a defect-free surface coating with a thickness of less than 1 μm was not possible. The work reported here details a new technique used for the formation of thin (< 1 μm) dense-skinned organic–inorganic composite membranes. The inorganic support has potential advantages in its chemical and thermal stability while introducing negligible transport resistance. Potential applications for this type of composite include pervaporation and high temperature gas separations where conventional polymer supports tend to show insufficient environmental stability.

Composite membranes have been utilized primarily for water desalination work. These membranes typically have porous polymeric supports with a dense surface film of a second polymer type.

* To whom correspondence should be addressed.

Journal of Applied Polymer Science, Vol. 46, 1927–1938 (1992)
 CCC 0021-8995/92/111927-12

A wide variety of techniques have been reported for the production of these composites.[1-5] However, all of the techniques reported have the following in common:

1. The porous supports used typically have less than 5% surface porosity.[6]
2. The effective surface pore size of the support is generally less than 50 Å.
3. The tortuosity of the gas flow path is significantly greater than 1 and is more probably on the order of 4 to 5.
4. The resistance introduced by the support is significant for gas separations and may present a measurable resistance for liquid separations as well.[7]

A few recent reports have documented the production of polymer–ceramic composite membranes. Liu and co-workers have reported the production of organic surface layers on ceramic supports by a complex electrochemical synthesis.[8] The technique is limited in its applicability by virtue of its complexity and the number of monomers that are suitable for this type of polymerization. Further, no measure of the degree of polymer layer perfection is provided. Finally, a report from Wilson et al., describes the production of polymer–ceramic composite membranes using dip and spray coating techniques.[7] Dense films with a thickness of approximately 0.5 μm are reported. Testing for liquid separation indicated that the films were essentially defect-free. However, the inability to produce spray droplets that were smaller than approximately 1 μm in diameter has precluded the use of spray coating for the production of uniform film coatings that are both defect-free and have thicknesses of less than 1 μm.[9]

While these techniques have been acceptable, several limitations exist with their use. The most serious are the inability to produce *ultrathin defect-free* surface coatings and the inability to use supports that have negligible resistance to gas flow. The supports used for conventional dip coating have contained relatively small complex pores in order to limit the migration of polymers into the pores of the support. Yet, these supports provide unwanted resistance to gas flow. In contrast, the technique reported here provides an approach to minimize these concerns.

The technique described in this work considers the formation defect-free dense-skinned polymer–ceramic composite membranes with thicknesses of less than 1 μm. The polymer layer has been applied by a solution deposition method that provides direct control of the ultimate polymer layer thickness. By proper choice of the polymer material, composites can be prepared on supports that have pores as large as 200 Å in diameter with an effective tortuosity of unity. These supports are sufficiently porous to produce a negligible contribution to the resistance of the composite membrane. These composites have the mechanical strength of a ceramic material with the inherently high selectivity of a glassy polymer.

EXPERIMENTAL

Materials

Polymers

The polymers used for the production of the dense organic separating layer are shown in Figure 1. The majority of the work reported here was completed using a fluorinated dianhydride-diamine, 5,5′-[2,2,2-trifluoro-1-(trifluoromethyl)ethylidene]bis-1,3-isobenzofuran-dione, isopropylidenedianiline (6FDA-IPDA). Other polymers were studied to establish the generality of the technique. These polymers were bisphenol-A polycarbonate (PC), tetrabromohexafluorobisphenol-A polycarbonate (TBHFPC), tetramethylhexafluorobisphenol-A polycarbonate (TMHFPC), tetramethylhexafluoropolysulfone (TMHFPSF), and 5,5′-[2,2,2-tri-fluoro-1-(trifluoromethyl)ethylidene]bis-1,3-isobenzofuran-dione, methylenedianiline (6FDA-MDA). The polymers were either synthesized in our labs[10,11] or supplied by the commercial labs of Boron Biologicals and Bayer. All materials were used without further purification or fractionation.

Physical characterization in terms of polymer density in the bulk state and glass transition temperature of these materials is provided in Table I. Macroscopic densities were measured in a density gradient column. Glass transition temperatures (T_g) were measured using a Perkin-Elmer DSC7 at 20°C per minute.[10-12]

Calculated values of the hydrodynamic diameter of each polymer in the solutions used are presented in Table II. Calculations were based on the retention time measured from a gel permeation chromatograph and the Einstein viscosity law[13]:

$$[\eta]M = KV \qquad (1)$$

where $[\eta]$ is the intrinsic viscosity of the polymer solution (dL/g), M the molecular weight, K a con-

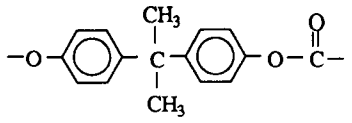

Bisphenol - A Polycarbonate (PC)

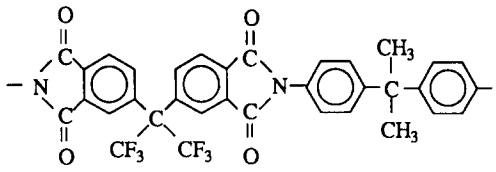

6FDA - IPDA

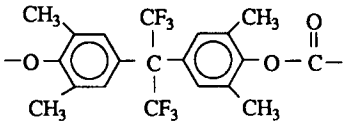

Tetramethylhexafluoro
Bisphenol - A Polycarbonate (TMHFPC)

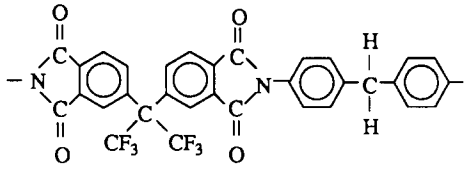

6FDA - MDA

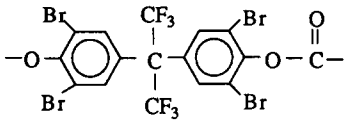

Tetrabromohexafluoro
Bisphenol - A Polycarbonate (TBHFPC)

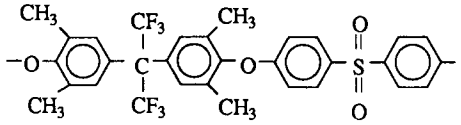

TetramethylhexafluoroPolysulfone (TMHFPSF)

Figure 1 Structure of polymers studied.

stant, and V the hydrodynamic volume of the polymer coil. Grubisie et al.[13] demonstrated the generality of this equation by producing a "universal" calibration for a given set of columns using a variety of linear, branched, and star-shaped polymers. They demonstrated that independent of polymer type or chemical nature, a single constant, K, could be used in Eq. (1).

For linear polymers, the hydrodynamic volume of the polymer coil can be related to the root-mean-square end-to-end distance of the polymer coil through the following equation proposed by Flory:[14]

$$[\eta]M = \Phi(h^2)^{3/2} \tag{2}$$

where Φ is the universal constant quoted by Billmeyer[15] as 2.8×10^{21} and $(h^2)^{1/2}$ is the root-mean-square end-to-end distance of the polymer coil.

Polymer molecules take on numerous configurations in solution. We can, however, speak of the average properties of the material. Even for the relatively stiff-chained polymers studied here, if it is assumed that the polymer molecule assumes a spherical configuration, the diameter of the sphere, d_h, can be estimated using the following relations:[16]

$$(h^2)^{1/2} = (6)^{1/2}R_g \tag{3}$$

and

$$d_h = 2R_g \tag{4}$$

Table I Physical Properties of Polymers

Polymer	Density (g/cm^3)	T_g (°C)	Ref.
6FDA-IPDA	1.352	310	11
6FDA-MDA	1.400	304	11
PC	1.200	150	10
TBHFPC	1.987	255	10
TMHFPC	1.286	208	10
TMHFPSF	1.286	243	12

Table II Molecular Volume of Polymers[a]

Polymer	GPC Retention Vol (cm^3)	$[\eta]M_w$	$[\eta]_{THF}$ (dL/g)	$[\eta]_{MC}$ (dL/g)	d_{THF}[c] (Å)	d_{MC}[d] (Å)
6FDA-IPDA	27.6	39233	0.41	0.38	197	192
6FDA-MDA	26.3	98175	0.42	0.27	267	230
PC[b]	30.8	4023	0.71	—	92	—
	26.0	121320			287	
TBHFPC	28.5	20790	0.15	0.19	160	173
TMHFPC	25.4	185260	—	—	330	—
TMHFPSF	26.0	121320	0.42	0.39	287	280
Polystyrene (M = 15K)	32.0	176	0.12			
Polystyrene (M = 470K)	23.7	614760	1.31			
Polystyrene (M = 200K)	25.8	139700	0.72			

[a] Viscosity references: Polysytrene[25]; all others measured by authors.
[b] The PC sample had a bimodal distribution with the major peaks as shown. Ratio of peak area ~ 1/1.
[c] Diameter of swollen polymer coil in THF.
[d] Diameter of swollen polymer coil in methylene chloride.

where R_g is the radius of gyration of the polymer coil.

Using the approximation of a spherical geometry, the hydrodynamic diameter of each polymer in solution was calculated. The results are presented in Table II. These results show that the hydrodynamic diameter is a function of the power of the solvent used, as would be expected. Because the functionality between hydrodynamic volume (solvent power) and hydrodynamic diameter is a cubic one, the small change in solvent power from tetrahydrofuran to methylene chloride produces only a minor change in the diameter of the swollen polymer chains.

Gel permeation chromatography was completed on each polymer and on three polystyrene standards using ~ 0.2 wt % polymer solutions in tetrahydrofuran and a Waters Ultrastyragel® column. The retention time of polystyrene standards with molecular weights of 15,000 and 470,000 were used to produce a calibration curve for the particular chromatograph used. The third standard was run to check the accuracy of this calibration. The reported molecular weight of the third standard was 200,000. The molecular weight measured by chromatography was approximately 192,000, an error of approximately 6%. Using the calibration curve, the product of intrinsic viscosity in THF and molecular weight was calculated for each polymer. The intrinsic viscosity in tetrahydrofuran and methylene chloride for each polymer was measured using an Ostwald-Fenske viscometer and solution concentrations of 0.1 to 1.0 g/dL. All viscometry measurements were made at 25°C. Insufficient material was available to complete viscometry measurements on the TMHFPC.

The PC sample exhibited a bimodal distribution in hydrodynamic volume. The ratio of the areas of the two peaks was ~ 1/1. The ramifications of this bimodality will be discussed further in the results section.

Solvents

Reagent-grade methylene chloride, purchased from Fisher Scientific, was used without further purification. HPLC grade tetrahydrofuran, purchased from Aldrich, was used as a carrier for gel permeation chromatography. The THF was degassed by sparging the solvent with helium for a period of at least 5 min. The degassed THF was used without further purification.

Ceramic Supports

Microporous Anopore™ aluminum oxide filters prepared by Anotec Separations with an average surface pore diameter of 200 Å and a bulk pore diameter of 2000 Å were used as the support. The Anopore™ inorganic membrane has a highly ordered "honeycomb" structure of capillary pores,[17] which are essentially cylindrical and straight. These asymmetric membranes exhibit a high porosity and low tortuosity producing low resistance to gas flow. These membranes were used as received without further treatment.

Gases

Compressed gases with purities of greater than 99.9% were purchased from Linde and used without

further purification. Oxygen, nitrogen, and helium were used as test penetrants.

Membrane Preparation

Composite membranes have been prepared by the deposition of a thin selective polymer layer on a microporous ceramic support. Dilute solutions of 0.1–1 wt % polymer in methylene chloride were prepared by mixing the polymer and solvent in a sealed bottle on a mechanical stirring plate. These solutions were allowed to mix for a minimum of 1 h. As the solvent is relatively volatile at atmospheric conditions, the solutions were used within a few days of preparation. The evaporation rate of the solvent was monitored from the "stock" solution and the approximate new concentration of the solution calculated prior to each use. Evaporation rates were monitored by direct measurement of the volume of solution present and by measurement of the weight of the solution to allow accurate thickness control of the composite layer thickness. Although it was not absolutely necessary to filter the solutions to obtain defect-free membranes, filtration appears to minimize the probability of producing defects and aids in the process of membrane formation. Therefore, many of the solutions were filtered through Teflon® filters with a sieving diameter of 0.45 μm prior to use.

The ceramic supports were placed on a clean glass sheet. A measured volume of solution was applied directly to the support. This forming polymer–ceramic composite membrane was then maintained in a solvent-saturated environment. By direct control of the solvent concentration of the surrounding air, the rate of evaporation of solvent from the polymer solution was controlled. This allows the polymer chains to be transformed very slowly from a swollen and expanded state after deposition to the equilibrium interpenetrated state in the ultimate composite. A fast transition between the two states is not optimum because the ceramic support is not flexible and rapid evaporation induces stresses in the ceramics that can ultimately fracture under the load from the high modulus coating.

The nascent membranes were maintained in a saturated solvent environment from 30 min to 2 h and then air dried in a 25°C room for a minimum of 6 h. Samples were then dried in a vacuum oven at 100°C for a period of at least 1 h prior to testing.

Gas Permeation Experiments

The permeability and selectivity properties of the composite membranes produced were measured using pure gas flux measurements. A membrane area of 15.2 cm^2 was used for all measurements. This area corresponds to the exposed surface area for the composite membrane. As the ceramic support is composed of pores that provide minimal resistance to gas flow and amorphous ceramic that is essentially impermeable to gas, the assumption of an area for permeation equal to the total surface area of the membrane may not be completely correct. However, applying the analysis developed by Keller and Stein[18] to this situation results in an estimated error associated with this approximation of less than 3% if the thickness of the film is greater than 1000 Å. For thicker films, the error decreases accordingly.

Pure gases were applied to the upstream side of the membrane at a fixed pressure, typically 50 psig. The volumetric gas fluxes were measured using a soap-bubble flow meter. Measurements were completed using a Millipore® test cell at 25°C and atmospheric pressure downstream unless otherwise noted. A few tests were completed using a vacuum cell employed in our labs.[19] These tests were run with a permeate pressure of less than 10 torr with variable upstream pressure. These tests were completed at 35°C.

Permeation through single-layered composites has been described by several researchers.[20-23] This series resistance model has been applied to flow through a dense polymer film and a porous ceramic support. For a composite membrane, governing equations for gas flux and selectivity are as follows:

$$N_i = \frac{\Delta p}{L_{\text{Ceramic}}/P_{\text{Ceramic } i} + L_{\text{Poly}}/P_{\text{Poly } i}} \quad (5)$$

where N_i is the volumetric flux of gas i through a membrane of known area, Δp is the pressure difference between the upstream and downstream side of the membrane, L_{Poly} is the polymer layer thickness, L_{Ceramic} is the ceramic layer thickness, $P_{\text{Poly}\,i}$ and $P_{\text{Ceramic}\,i}$ are the permeability of gas i through the polymer and ceramic layer, respectively.

The ideal selectivity of the composite membrane, $\alpha_{A/B}$, is equal to the ratio of permeation rates of pure gases A and B measured under equal pressure driving force; therefore,

$$\alpha_{A/B} = \frac{N_A}{N_B} \quad (6)$$

When the resistance of the composite membrane to gas permeation lies primarily within the polymer layer, the selectivity of the composite membrane reduces to

$$\alpha_{A/B} = \frac{P_{\text{Poly A}}}{P_{\text{Poly B}}} \tag{7}$$

For this case of minimal resistance in the support, the pressure-normalized flux of gas i permeating through a membrane is given by

$$\left(\frac{P}{L}\right)_{\text{Poly } i} = \frac{N_i}{\Delta p} \tag{8}$$

The effective skin layer thickness of a defect-free composite membrane is given by

$$L_{\text{Poly}} = \frac{P_i}{(P/L)_{\text{Poly } i}} \tag{9}$$

where P_i is the permeability coefficient of gas i, as determined on thick, isotropic films of known thickness.

RESULTS AND DISCUSSION

Gas Flux Measurements

The resistance to gas flow was measured for both the ceramic support and for the composite membranes produced. For the ceramic support membranes, the flux of helium, oxygen, and nitrogen were all greater than 10,000 GPU (1 GPU = 10^{-6} cm^3 (STP)/cm^2 cm Hg). These flux rates are sufficiently high to cause no measurable resistance in the polymer–ceramic composite membranes.

Pure gas permeation rates were measured for each of the composite membranes tested. The pressure normalized flux for each membrane was calculated for each test using Eq. (8). The separating ability of a membrane was measured by calculating the selectivity of the membrane for a given gas pair using Eq. (6).

The majority of the work presented in this study is based on the polyimide, 6FDA-IPDA. Results achieved with this polymer are presented in Table III. There, gas fluxes and selectivities for selected gas pairs are presented. Also presented in Table III are the permeabilities and selectivities for a dense isotropic film of the polymer at 25°C as determined by the authors. Dense film properties were obtained from gas flux measurements at 35°C and activation energies measured over the range of 35–70°C.

As the starting solution concentration of polymer increases, the data in Table III indicate that the thicknesses of the polymer layer increases accordingly although there is some scatter in the data. The results further indicate that selective composite membranes produced from this material can have nitrogen fluxes of as great as 8.4 GPU with an oxygen/nitrogen selectivity of 4.6. In our work, a membrane is defined as "selective" if it has measured selectivities of greater than 85% of the dense film values. The nitrogen flux rate (i.e., membrane thickness) can be controlled over the range of 0.7–8.4 GPU by proper choice of the casting solution concentration.

Results for the polycarbonates, polysulfone and the 6FDA-MDA are not as extensive as those for

Table III Gas Flux Results for 6FDA-IPDA Composite Membranes

Polymer Conc. (wt %)	Gas Flux N_2	Gas Flux O_2 (GPU)	Gas Flux Helium	Gas Selectivities O_2/N_2	Gas Selectivities He/N_2	Gas Selectivities He/O_2	L[a] (μm)
0.11	8.4	38.2	276.8	4.6	33.0	7.2	0.16
0.12	6.3	28.5	192.6	4.5	30.6	6.8	0.21
0.20	2.9	15.0	117.5	5.2	40.5	7.8	0.45
0.32	3.1	14.6	101.2	4.7	32.7	6.9	0.42
0.35	3.7	18.0	105.2	4.9	28.4	5.8	0.35
0.43	1.2	5.4	40.5	4.6	33.7	7.5	1.08
0.45	1.6	7.6	47.3	4.8	29.6	6.2	0.81
0.67	1.1	5.6	41.7	5.1	37.9	7.4	1.18
1.20	0.7	3.5	—	5.0	—	—	1.86
Dense film permeability[a]/ selectivity	1.3	6.7	59.2	5.1	45.5	8.8	

[a] Permeabilities in barrers. 1 barrer = 1×10^{-10} (cm^3 cm)/(cm^2 cm Hg s). Film thickness calculated using dense film permeability for nitrogen.

the 6FDA-IPDA; however, they indicate the ability to produce defect-free composite membranes from high molecular weight samples of these materials (see Table IV). The gas separating characteristics of dense polymer films of each polymer are also reported in Table IV at 35°C. The data reported in Table IV indicate that selective composite membranes were produced from the TMHFPC, TMHFPSF, and the 6FDA-MDA materials studied.

For composite membrane formation using these various polymers, solutions corresponding to calculated film thicknesses of approximately 0.5 μm were used. The data for the three selective composite membranes indicate that the measured thickness for each of the polymers was between 0.28 and 0.91 μm. The difference between the measured and calculated thickness will be discussed in further detail at a later point.

The PC and TBHFPC samples used here did not produce selective composite membranes; however, their data are reported for comparison to support the points regarding the importance of controlling the relative size of surface pores and hydrodynamic diameters of dissolved macromolecules used in such applications.

Further attempts to produce a defect-free polymer layer using these materials were not successful. Recoating the defective composite membranes with a second or third polymer layer decreased the gas flux through the membrane, but the selectivity for oxygen/nitrogen did not increase above ~ 3.0 for the PC even when the film thickness calculated from gas flux measurements was as great as 4 μm. If even a small fraction of the pores remain unobstructed by polymer, the selectivity of the composite may be significantly less than that of the defect-free polymer layer alone.[24]

Based on the data in Table II, both the TBHFPC and the PC samples used here had average hydrodynamic diameters that were smaller than the other polymers tested. The TBHFPC had a measured average chain diameter of 173 Å, which was insufficient to produce defect free coatings on the 200 Å nominal pore size of the support. It is even less surprising that defect-free composite membranes were not produced from the PC since this sample had a very wide distribution of molecular diameters, ranging from ~ 90 to ~ 290 Å. This wide distribution made it possible for some of the material to migrate into the pores of the support. While the results indicate that the resistance to gas flow increased significantly over the uncoated membrane, the selectivity of the dense isotropic film was not achieved.

The other polymer samples used that had measured coil diameters of ~ 200 Å or greater were all of sufficient molecular size for the swollen polymer chains to be excluded from the pores of the support. These materials produced essentially defect-free surface coatings.

By proper control of the molecular weight of the polymers used and the solvent selected, the hydrodynamic diameter of the polymers in the swollen state can be maintained at a level which is larger than the pore size of the underlying support. There-

Table IV Gas Flux Results for Other Polymer Composite Membranes

Polymer	Film Type (Composite or Dense)[a]	Gas Flux or Permeability (N_2) (GPU or Barrer)	Gas Flux or Permeability (O_2) (GPU or Barrer)	Gas Flux or Permeability (Helium) (GPU or Barrer)	Gas Selectivities O_2/N_2	Gas Selectivities He/N_2	Gas Selectivities He/O_2	L[a] (μm)	Ref.
6FDA-MDA	Composite	2.9	14.4	125.3	5.0	43.2	8.7	0.28	
6FDA-MDA	Dense	0.8	4.6	50.0	5.7	61.7	10.9		11
PC	Composite	16.2	15.5	—	1.0	—	—	—[b]	
PC	Dense	0.3	1.6	13.0	4.9	39.4	8.1		26
TBHFPC	Composite	364.0	400.0	473.0	1.1	1.2	1.3	—[b]	
TBHFPC	Dense	1.8	9.7	100.0	5.4	55.6	10.3		10
TMHFPC	Composite	12.9	52.2	262.9	4.0	20.4	5.0	0.60	
TMHFPC	Dense	7.8	32.0	200.0	4.1	25.6	6.3		26
TMHFPSF	Composite	4.8	22.3	142.7	4.7	29.7	6.4	0.91	
TMHFPSF	Dense	4.0	18.0	113.0	4.5	28.3	6.3		12

[a] Film type: "Composite" indicates composite membrane, "Dense" indicates dense film. Gas flux corresponds to composite membrane data, permeability corresponds to dense film data. Fluxes are reported in GPU: 1 GPU = 1×10^{-6} $cm^3/(cm^2\ cm\ Hg\ s)$; permeabilities are reported in barrers: 1 barrer = 1×10^{-10} $cm^3\ cm/(cm^2\ cm\ Hg\ s)$. Polymer film layer thickness calculated using dense film nitrogen permeability.

[b] These composite membranes were defective and no meaningful thickness for a "defect-free" polymer layer can be calculated.

fore, the polymer chains are sieved out of the solution as it flows through the ceramic support. Thus, only the polymer chains that are larger than the pore openings of the ceramic are excluded. If the polymer chains are smaller than the pore opening of the ceramic, they can simply flow into the support. Because the volume of polymer applied to each support is limited to the amount required to produce a controlled surface coverage, if even a few percent of the polymer flows into the support, the material left for surface coverage may be insufficient to produce a defect-free layer.

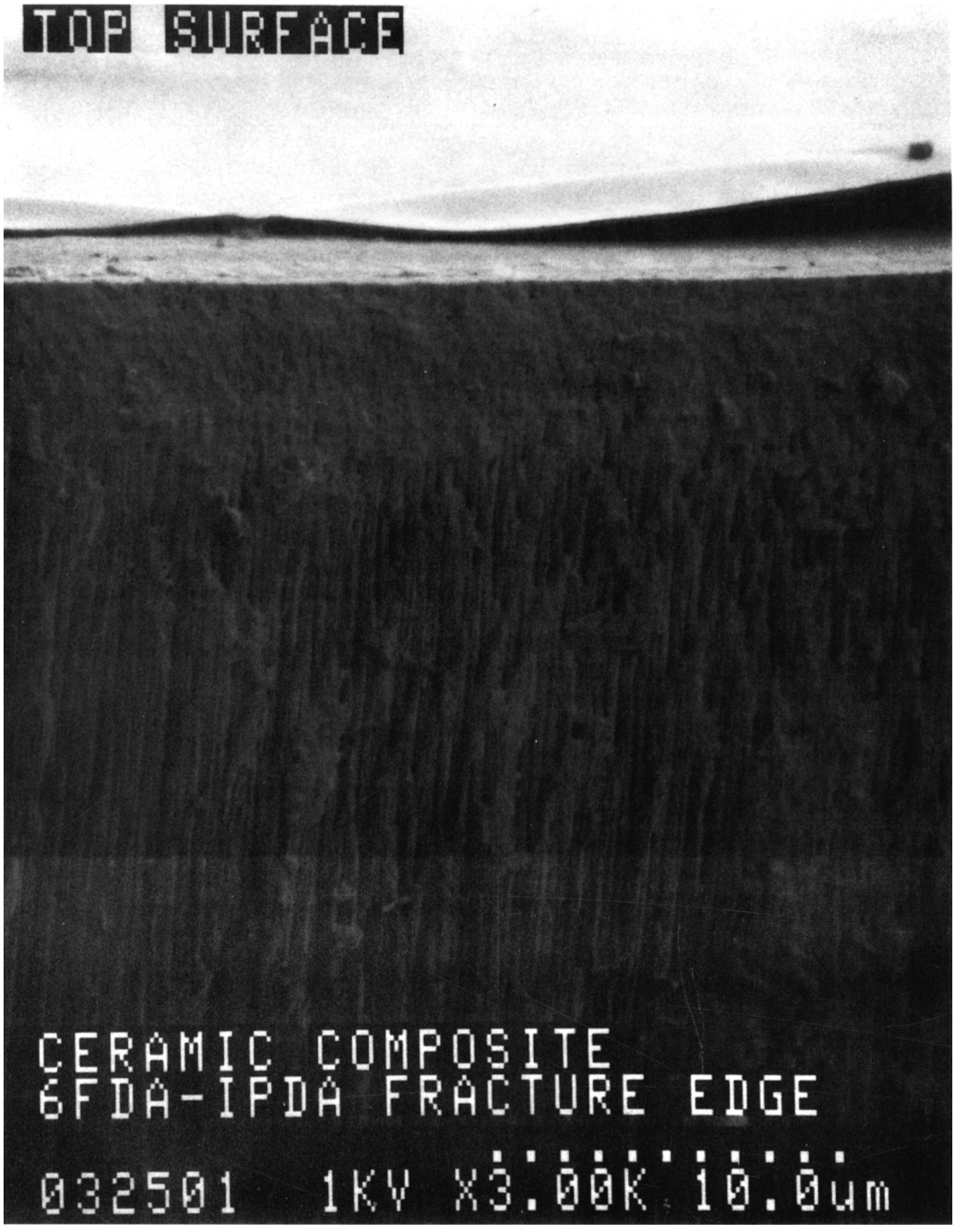

Figure 2 Scanning electron micrograph of the cross section of a fractured 6FDA-IPDA composite membrane. Potograph taken at a magnification of 3000× and 1 kV.

Scanning Electron Micrographs

Scanning electron micrographs have been produced for a number of samples. Cross sections of a 6FDA-IPDA composite membrane are presented in Figures 2 and 3. Figure 2 provides a view of both the ceramic support and the thin polymer layer. Figure 3 is a more highly magnified view of the supported polymer. Several interesting characteristics are observed in these micrographs. First, the thickness of the polymer layer can be estimated from Figure 3 as 1800 Å. Further examination of this photograph in-

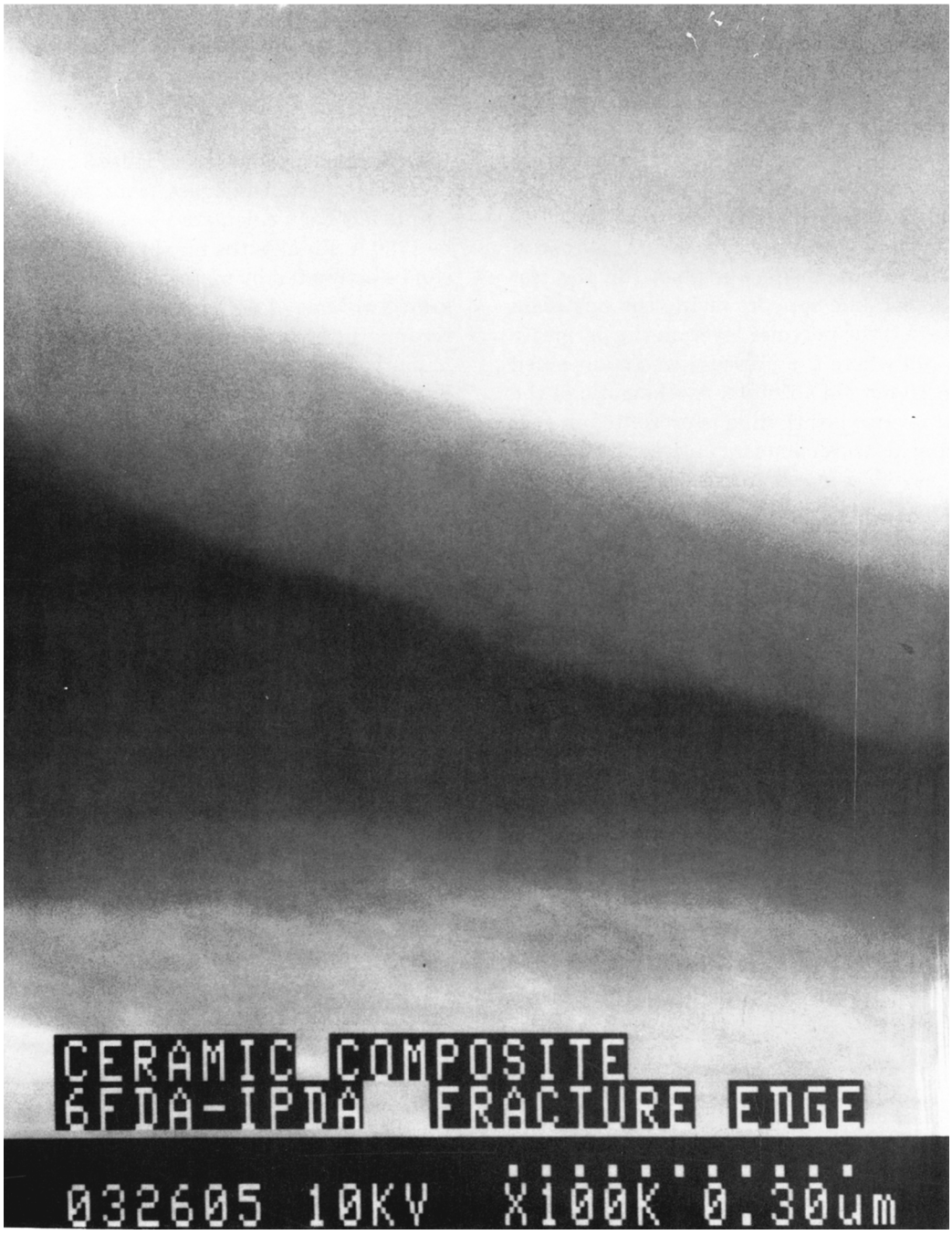

Figure 3 Magnified view of the scanning electron micrograph of the cross section of the composite membrane shown in Figure 2. Potograph taken at a magnification of 100,000× and 10 kV.

dicates that the polymer is a dense mass with no obvious void space present. By examining Figure 2, it is obvious that the layers are discrete. No polymer impregnation is seen in the pores of the support ceramic. Finally, a discontinuity is seen between the two layers. Upon preparing the composite for photography, the membrane was frozen in liquid nitrogen and stress fractured. This resulted in the polymer layer being pulled away from the ceramic support. No apparent problems were encountered in our work with delamination. We expect, therefore, that the extreme conditions of cryofracturing are likely to be responsible for the apparent delamination.

To evaluate the physical integrity of the polymer–ceramic interface, gas permeation experimentation was completed. First, the composite was tested in the normal fashion to determine gas flux characteristics. Then, the composite was placed in the test cell with the ceramic support facing the upstream gas pressure and the polymer layer on the permeate side of the cell where the pressure was maintained at less than 10 mmHg absolute. A schematic of the normal and reverse positioning is presented in Figure 4. Gas flux measurements for both configurations completed at 75 psia upstream were equivalent within the experimental error of the system. This indicated that the membrane was indeed intact when the pressure was applied to the ceramic side of the composite. If the polymer layer was to delaminate, one would expect that gas would bypass the polymer layer, travel around the edge of the polymer layer and increase the measured flux rates. Further, the gas separating ability of the membrane would be lessened. These phenomenon were not observed. Conversely, the gas separating factor of the composite membrane was independent of the configuration of the experiment.

Estimation of Skin Layer Thickness

Skin layer thickness has been estimated from scanning electron microscopy, gas flux measurements, and material balance calculation. Using scanning electron microscopy, the thickness of the 6FDA-IPDA composite shown in Figure 3 can be estimated as 1800 Å. The thickness from gas flux measurements has been calculated by evaluating Eq. (8) to be 1780 Å. Finally, the maximum thickness possible can be estimated by material balance calculation. A known volume of polymer solution is applied to the ceramic filter of known area; therefore, the maximum thickness achievable can be directly calculated. For the sample in question, this thickness is 4500 Å. The values from these three techniques are somewhat varied. However, the two measured values are in quite good agreement. Further, both of these values are below the calculated maximum as would be expected.

The maximum achievable thickness for each of the selective 6FDA-IPDA samples as calculated from material balance is presented versus the measured thickness from gas permeation in Figure 5. While a

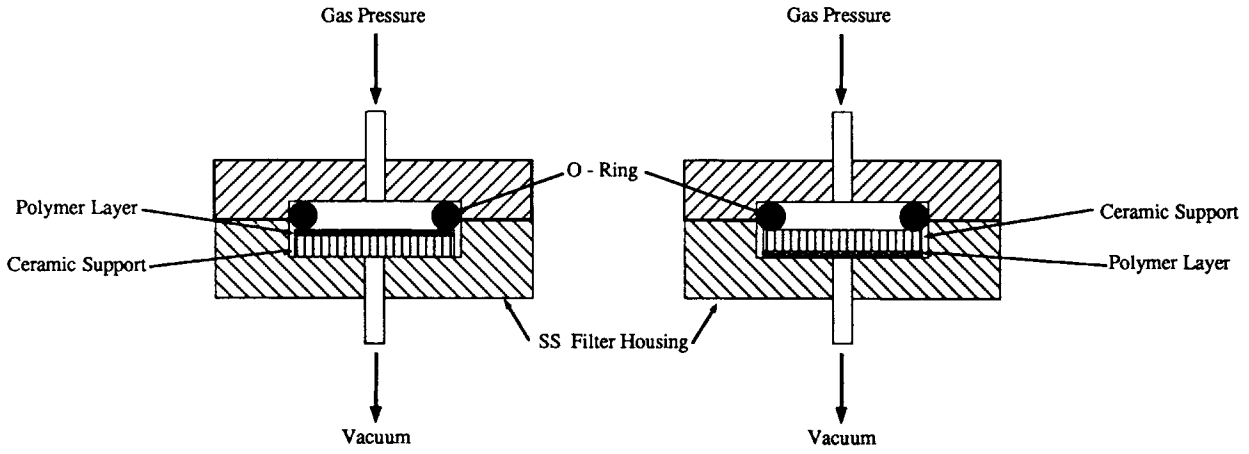

Figure 4 Membrane orientation used to evaluate the potential for delamination in the composites. "Normal" position used for regular gas permeation testing. "Reverse" position used only to measure the strength of the polymer–ceramic interface.

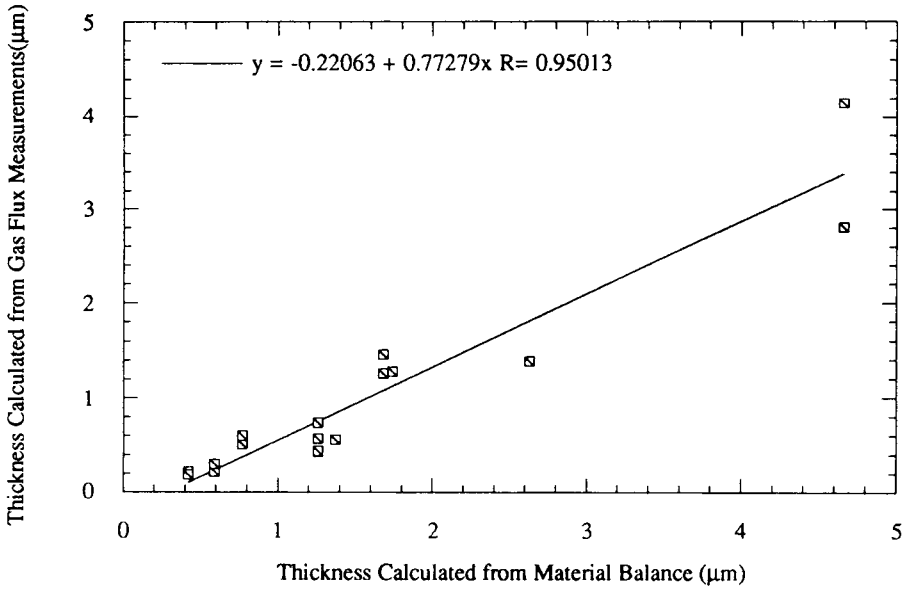

Figure 5 Correlation between the thickness calculated from gas flux measurements and the maximum thickness calculated from material balance. Data represents 6FDA-IPDA samples with selectivities of >90% the intrinsic value.

good correlation exists, the measured thickness is consistently less than the maximum material balance calculated value. On the average, the measured value is approximately 20% less than that calculated from material balance. The difference observed in these values may be due to the loss of polymer during the application step; however, other cumulative contributions may also be at play to explain the discrepancy. Among these is the possibility that adsorbed water or residual volatiles present in the polymer powders are removed during final film drying along with the solvent. As all solutions were prepared on a weight basis, any additional weight from sorbed species would result in a shift of the kind indicated. The extent of discrepancy between the calculated and measured thicknesses are, however, considerably greater than would be expected due to even a 3–5% error of this type. A more likely possibility was expected to be due to penetration of the lower molecular weight fractions (lower hydrodynamic diameters) into the pores of the substrate. The polymer necessary to create a discrepancy as great as 2000 Å in the surface thickness could produce a fine coating along the surface of the pores that had an average thickness of less than 8 Å. In all likelihood, this coating would not be evenly distributed. Instead, it is believed that the coating would be thickest at the entrance to the pore and decrease exponentially along the pore length. This point is under further investigation.

Further examination of Figure 5 indicates that the correlation does not intercept the origin as might be expected. Yet, further consideration of this question leads us to the conclusion that there is some absolute minimum volume of polymer that is required to be applied prior to the development of a defect-free layer. At very low volumes of polymer applied, it is possible to produce a fairly uniform coverage that still contains some defects. If these defects cover more than a few percent of the surface, the pressure-normalized flux (P/L) measured for this membrane will be substantially greater than that measured for a defect-free coating of equivalent thickness. Therefore, the thickness calculated from the gas flux measurement will be nearly zero [see Eq. (9)] while the thickness from material balance may be as great as a few hundred angstroms. This trend of near-zero thickness measured from gas flux and a nonzero value measured from material balance will continue until enough polymer is applied to the surface to produce a defect-free coating. Once a defect-free coating is formed, the agreement between the two values is significantly improved. The two values will be equivalent if the errors discussed in the previous paragraph are not present. Therefore, the nonzero intercept of the correlation presented in Figure 5 is the result of defective surface coatings at very low volumes of polymer applied and the penetration of polymer coils with small hydrodynamic diameters into the pores of the support.

CONCLUSIONS

Ultrathin, highly productive polymer–ceramic composite membranes can be prepared by a solution deposition technique. The membrane formation mechanism believed to be occurring is one of molecular-scale sieving of macromolecular chains by the almost monodispersed 200 Å pores in the surface of the ceramic membrane. Polymers with swollen chain diameters that are larger than the underlying pores of the ceramic support are sieved out of solution, while the solvent is allowed to pass through the ceramic and evaporate. Polymers that had swollen chain diameters smaller than that of the ceramic pore were able to pass into the pores of the support and defect-free films were not produced. This technique has been used to produce polymer-ceramic composite membranes with a controlled skin layer thickness for a variety of polymers.

The authors would like to thank Dr. Ingo Pinnau, Mr. Peter Pfromm, and Mr. Johann Le Roux for valuable suggestions during the course of this work; Dr. Mark Hellums for supplying polymer samples and Mr. Ken Achacosa for technical assistance.

This material is based in part upon work supported by the Governor's Energy Management Center—State of Texas Energy Research in Applications Program under Contract No. 003658-101.

REFERENCES

1. P. H. Carnell and H. G. Cassidy, *J. Polym. Sci.*, **9,** 1863 (1961).
2. R. L. Riley, H. K. Lonsdale, C. R. Lyons, and U. Merten, *J. Appl. Polym. Sci.*, **11,** 2143 (1967).
3. R. L. Riley, H. K. Lonsdale, and C. R. Lyons, *J. Appl. Polym. Sci.*, **15,** 1267 (1971).
4. R. Schucker, U.S. Pat. 4,837,054 (1989).
5. R. Schucker, U.S. Pat. 4,861,628 (1989).
6. H. Strathman, "Synthetic Membranes and their Preparation," in *Handbook of Industrial Membrane Technology,* M. C. Porter, Ed., Noyes Publications, Park Ridge, NJ, 1990.
7. I. Wilson, L. D. Nelson, D. T. Friesen, S. B. McGray, and R. C. Furneaux, *International Congress on Membranes,* 1191 (1990).
8. C. Liu, M. W. Espenscheid, W. J. Chen, and C. R. Martin, *J. Am. Chem. Soc.*, **112,** 2458 (1990).
9. S. M. Lee, *Encyclopedia of Chemical Technology,* Vol. 10, 1978, Wiley, New York, pp. 247–283.
10. M. W. Hellums, Ph.D. Dissertation, The University of Texas at Austin (1990).
11. T. H. Kim, Ph.D. Dissertation, The University of Texas at Austin (1987).
12. J. S. McHattie, Ph.D. Dissertation, The University of Texas at Austin (1990).
13. Z. Grubisie, P. Rempp, and H. Benoit, *Polym. Lett.*, **5,** 753 (1967).
14. P. J. Flory, *Principles of Polymer Chemistry,* Cornell Univ., Ithaca, NY, 1953.
15. F. W. Billmeyer, Jr., *Textbook of Polymer Science,* 3rd ed., Wiley, New York, 1984.
16. D. W. Van Krevelen, *Properties of Polymers,* Elsevier Science Publishers, New York, 1990.
17. R. C. Furneaux, W. R. Rigby, and A. P. Davidson, *Nature,* **337,** 147 (1989).
18. K. H. Keller and T. R. Stein, *Math. Biosci.*, **1,** 421 (1967).
19. W. J. Koros and D. R. Paul, *J. Polym. Sci. Polym. Phys. Ed.*, **14,** 1903 (1976).
20. J. M. S. Henis and M. K. Tripodi, *J. Memb. Sci.*, **8,** 233 (1981).
21. J. L. Lopez, S. L. Matson, J. Marchese, and J. A. Quinn, *J. Memb. Sci.*, **27,** 301 (1986).
22. I. Pinnau, J. G. Wijmans, I. Blume, T. Kuroda, and K. V. Peinemann, *J. Memb. Sci.*, **37,** 81 (1988).
23. K. A. Lundy and I. Cabasso, *Ind. Eng. Chem. Res.*, **28,** 742 (1989).
24. J. M. S. Henis and M. K. Tripodi, *Science,* **220,** 11 (1983).
25. M. Kurata, M. Iwawa, and K. Kamada, in *Polymer Handbook,* J. Brandrup and E. H. Immergut, eds., Wiley, New York, 1966.
26. M. W. Hellums, W. J. Koros, G. R. Husk, and D. R. Paul, *J. Memb. Sci.*, **46,** 93 (1989).

Received October 4, 1991
Accepted January 29, 1992